

Data-Driven Web-Based Patching Management Tool Using Multi-Sensor Pavement Structure Measurements

Sneha Jha¹, Yaguang Zhang², Bongsuk Park³, Seonghwan Cho⁴, James V. Krogmeier², Tandra Bagchi³, and John E. Haddock³

Transportation Research Record
2023, Vol. 2677(12) 83–98
© National Academy of Sciences:
Transportation Research Board 2023
Article reuse guidelines:
sagepub.com/journals-permissions
DOI: 10.1177/0361198123116716
journals.sagepub.com/home/trr


Abstract

Automating pavement maintenance suggestions systems is challenging, especially for actionable recommendations such as patching location, depth, and priority. It is a common practice among state agencies to manually inspect road segments of interest and decide maintenance requirements based on the pavement condition index (PCI). However, standalone PCI only evaluates the pavement surface condition which, coupled with the variability in human perception of pavement distress, limits the accuracy and quality of current pavement maintenance practices. In this case, there is a need for multi-sensor data integrated with standardized pavement distress condition ratings. This study explores estimating the appropriate pavement patching strategy (i.e., patching location, depth, and quantity) by integrating pavement structural and surface condition assessment with pavement ratings of distress. In particular, it combines pavement structural condition parameters and falling weight deflectometer deflections with surface condition parameters, international roughness index, and cracking density, for a better representation of overall pavement distress conditions. Then, a pavement-specific, threshold-based patching suggestion algorithm is designed to suggest pavement maintenance operations. The thresholds were determined based on a reliability concept and were verified with the structural number ratio. The threshold values were then used in the patching suggestion algorithm to create patching suggestion tables. A web-based Patching Management Tool (PMT) was designed as an interactive tool to visualize these patching suggestion maps and analyze the pavement distress data using geographical maps and graphs. The PMT was validated with road surface and right-of-way images obtained from three-dimensional laser sensors, and it could successfully capture localized distresses in existing pavements.

Keywords

pavement management system, patching management tool, falling weight deflectometer, international roughness index, cracking density

Introduction

Road networks are one of the largest continuous manufactured structures in active use and constitute a major portion of economic activities in the modern world. With increased traffic loads, road maintenance has only ever increased in scale. The Indiana Department of Transportation (INDOT), which maintains about 18,000 centerline kilometers of roads, invests billions of public-funded dollars on maintenance initiatives. Most state agencies rely on the experience of scoping engineers and experts to determine pavement maintenance strategies based on various pavement condition indices (PCIs).

However, the scale of maintenance and variability in human perception of pavement distress limits the implementation and maintenance strategies. To cover large

¹Department of Agriculture and Biological Engineering, Purdue University, West Lafayette, IN

²School of Electrical and Computer Engineering, Purdue University, West Lafayette, IN

³Lyles School of Civil Engineering, Purdue University, West Lafayette, IN

⁴Indiana Department of Transportation, West Lafayette, IN

Corresponding Author:

Seonghwan Cho, scho@indot.in.gov

areas of interest with better accuracy, automated pavement maintenance suggestion systems are in demand (1, 2). Pavement maintenance requirements involve more than the detection of localized distresses such as potholes, cracking, and faulting, because they must also account for various environmental factors, traffic loading, or both (3). Instead, pavement maintenance is grouped into three categories: preservation, rehabilitation, and reconstruction, based on low, medium, or high levels of pavement distress severity. The classification of pavement condition into these categories is based on thresholds. These thresholds are used to categorize the pavement into preservative, rehabilitative, or reconstructive maintenance requirement categories, but are often decided based on experience, human resources, time, and budget (3–7).

Surface patching, thin overlay, and structural overlay are typical methods used for the preservation and rehabilitation of pavements. These techniques use either visual distress indicators or decision trees based on the PCIs such as ride quality, pavement distress index, and so forth (8–10). PCI includes the international roughness index (IRI), rut depth, and crack density (CD) to classify pavement surface conditions (11–13). Vehicle-mounted IRI is an especially popular method of pavement assessment because of its ease of measurement and high resolution over long distances. Even though PCI is successful in characterizing pavement rideability, it does not properly account for the effect of pavement structural conditions.

Typically, the relation between the surface and structural conditions of the road is probabilistic, yet researchers have not been able to correlate the PCI and structural condition measurements (14, 15). The structural condition of the pavement is usually measured by the falling weight deflectometer (FWD), and the structural number index calculated from the FWD center deflection (16, 17). Although Sollazzo et al. have used neural networks and machine learning techniques to estimate the structural number index from IRI to predict pavement conditions (18), they do not yet relate to the overall structural condition. The structural condition of the pavement is better represented by the deflection basin parameters (DBPs), which reflect the layer condition at different depths in the pavement (19, 20).

Comprehensive pavement maintenance requires both surface and structural condition assessments. Thus, an information fusion of the surface and structural condition parameters is desirable to generate a comprehensive pavement condition assessment. Integrating the IRI, CD, and FWD measurement data spatially allows local distress detection and overall road structural condition using the high-resolution surface condition parameters and FWD DBPs, respectively. On these grounds, a complete patching suggestion based on a multi-sensor data fusion approach is proposed in this study.

Objective and Scope

This study's main objective is to develop a comprehensive patching suggestion tool by incorporating both functional and structural conditions of existing pavements into a threshold-based patching suggestion algorithm. To fulfill this objective, this study proposes a methodology to determine the threshold values of FWD, IRI, and CD parameters using current pavement condition measurements and local road conditions. This paper focuses on full-depth asphalt pavements, a typical pavement type in Indiana. For the current scope of the study, field FWD, IRI, and CD data were collected from the INDOT for all road classifications of full-depth asphalt pavements, that is, State Roads, US-Highways, and Interstate Highways. The collected field data were used to determine appropriate threshold values for the patching suggestion algorithm; the web-based application, Patching Management Tool (PMT) was created to visualize the suggested patching over a large network of roads.

Description of Pavement Condition Rating Parameters

The multi-sensor data fusion method for creating high-resolution patching suggestions spatially integrates pavement condition rating (PCR) parameters, IRI, and CD, measured from the three-dimensional (3D) laser imaging sensor, with pavement DBPs measured by FWD.

The IRI data used in this study were processed by commercial software, WayLink ADA3 (21, 22). This software can recalculate IRI for selected spatial resolutions and match the results with the road surface images obtained from the 3D laser imaging sensor and right-of-way (ROW) images. In this study, a 1.8 m length along the road was selected as the spatial resolution. The WayLink ADA3 software uses an improved crack-detection technique from 3D laser images using image processing and deep-learning neural networks (23). The crack-detection results provide a percentage of cracking on the left wheel path and right wheel path with the same spatial resolution as IRI.

FWD deflection parameters used in this study include two deflection values (D0 and D60) and three DBPs, which are used to evaluate the structural conditions of asphalt pavements (24). D0, the maximum deflection measured at the center of the FWD loading plate, is mostly used to assess the overall pavement structural conditions, whereas D60, the deflection measured at 1,500 mm from the loading center, represents the sub-grade condition. The three DBPs are surface curvature index (SCI), base damage index (BDI), and base curvature index (BCI). SCI is defined as the difference between D0 and D12 (deflection measured 300 mm from the loading center) and is used to characterize the structural

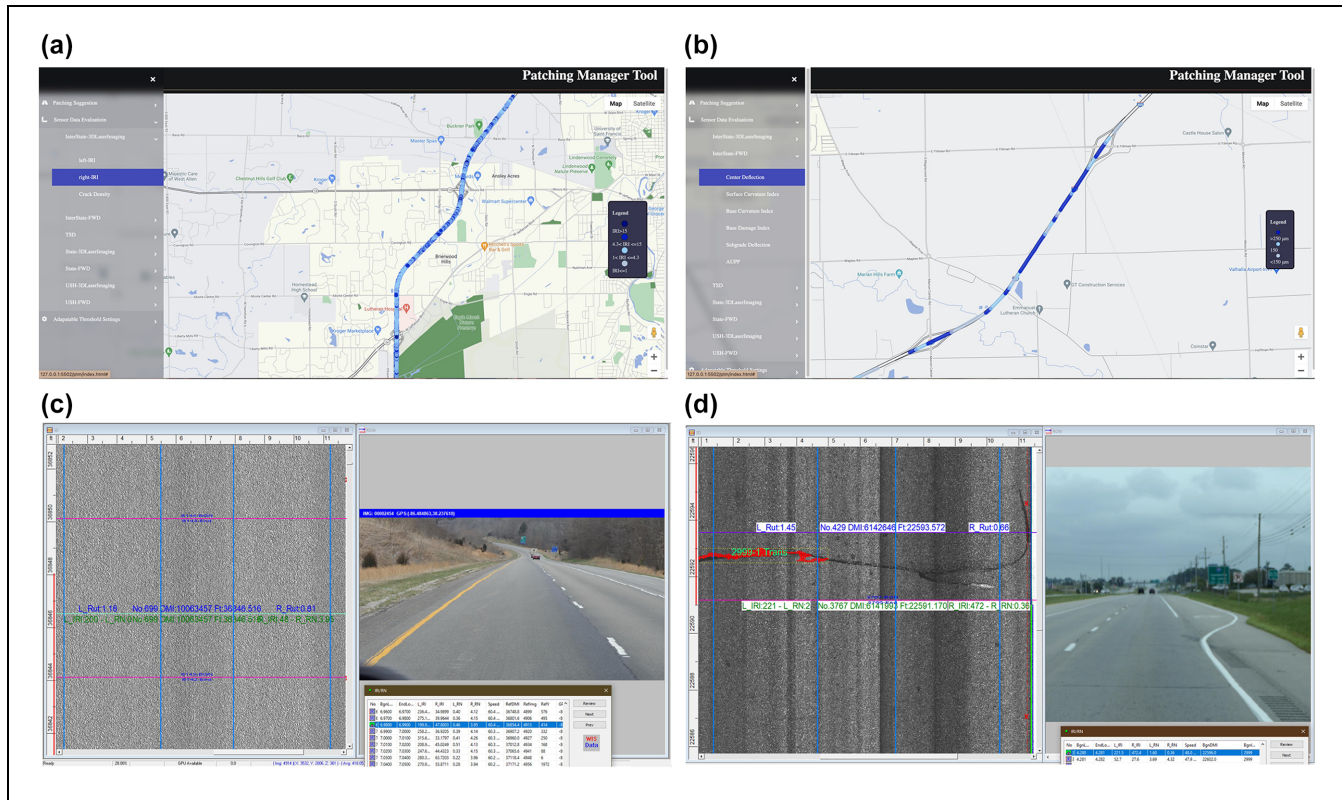


Figure 1. Example of visualized pavement condition rating: (a) international roughness index (IRI), (b) D0, (c) road surface image and right-of-way (ROW) image at the IRI measurement, and (d) road surface image and ROW image of transverse cracking.

conditions of pavement upper layers. BDI is the difference between D12 and D24 (deflection measured 600 mm away from the loading center), and BCI is calculated by subtracting D36 (deflection measured 900 mm away from the loading center) from D24. BDI and BCI are used to indicate the structural conditions of the base and sub-base layers, respectively. The use of DBPs as structural indicators allows us to determine appropriate patching depth by interpreting the structural conditions of each layer in full-depth asphalt pavements. Figure 1, *a* and *b*, shows examples of PCR parameters, IRI and D0 as visualized in the PMT web application interface. In addition, Figure 1, *c* and *d*, shows the road surface images and ROW images for each distance measurement instrument (DMI) number with 1.8 m spatial resolution obtained from the WayLink ADA3 software.

Determination of Thresholds for PCR Parameters

Determination of FWD Parameters Thresholds

Thresholds of FWD parameters were preliminarily determined based on the concept of design reliability, which is the probability of good pavement sections over the design period. According to the Mechanistic-Empirical

Pavement Design Guide, the reliability concept is recommended for determining performance threshold values to achieve a balance between maintenance costs and overall pavement structural health (25). In this study, a reliability analysis was conducted using the INDOT FWD database to determine preliminary thresholds of FWD parameters. As threshold values determined by the reliability concept are dependent on the current condition of the pavements, further verification was needed to determine whether the reliability-based approach can provide reasonable thresholds for the structural assessment of the pavements. Therefore, the prevalent structural condition index, structural number ratio (SNR), was used to verify the preliminary threshold values. This section describes the steps in the process of calculating the FWD parameter threshold values in detail, which include (i) determining the preliminary thresholds using the reliability, and (ii) verifying the preliminary thresholds using the SNR.

Determination of Preliminary FWD Thresholds Using Reliability. Two threshold values were selected to define three levels of pavement structural condition as good, fair, and poor. For each road classification, two reliability levels were selected at 5% intervals, based on the recommended level of reliability in the AASHTO 1993

design guide (26). Interstate Highways used 90% and 95% for lower and upper limits, US-Highways used 85% to 90% of reliability levels, and State Roads used 80% to 85%, respectively. As a road with heavier traffic typically requires a higher level of reliability, the highest reliability levels were selected for the Interstate Highway and the lowest for State Road. The higher reliability value was used as the threshold between poor and fair pavement conditions, whereas the lower reliability value was used as the threshold between fair and good pavement conditions. It should be noted that these reliability levels have been used and verified by previous researchers to determine thresholds of structural indicators (27, 28). Furthermore, similar percentage levels were observed and used by previous researchers to distinguish good and acceptable roads based on the IRI and ride quality index (29).

The FWD data collected from the INDOT pavement management system (PMS) database was used for reliability analysis. The total number of FWD data points was 1,579, 605, and 717 for State Roads, US-Highways, and Interstate Highways, respectively. The empirical cumulative distribution function (ECDF) was used to conduct the reliability analysis for determining preliminary threshold values of FWD parameters; it is an estimate of the cumulative distribution of each data point in the measured samples. To illustrate the role of ECDF, we have plotted the ECDF values against the FWD deflections, measured on Interstate Highway as shown in Figure 2. For example, the D0 values 214.9 and 149.1 microns correspond to the reliability levels 95% and 90%, meaning 95% of the D0 measurements are below 214.9 microns and 90% of the D0 measurements are below 149.1 microns among the total D0 measured on Interstate Highways in the scope of this study. Thus, we classify the Interstate Highway locations with D0 greater than 214.9 microns as poor road conditions. The same approach was applied to other FWD parameters as shown in Figure 2. The reliability results of FWD deflection parameters for the three distinct types of roads are summarized in Table 1. The values of the FWD parameter, corresponding to four reliability levels (80%, 85%, 90%, and 95%) are also presented in Table 1. Furthermore, it was found that the State Roads exhibited the greatest values of FWD deflection parameters, whereas the Interstate Highways showed the lowest values at the same reliability level. This is a reasonable trend because a conservative threshold value should be applied to the road with heavier and faster traffic (i.e., Interstate Highways) to maintain better conditions in comparison with State Roads or US-Highways, which have lower traffic volume. Similarly, the preliminary threshold values for all FWD deflection parameters are highlighted in Table 1.

Verification of FWD Thresholds Using the SNR. SNR is derived from the concept of a pavement structural number

developed by the American Association of State Highway Officials (AASHO), and it has been widely used in PMS to evaluate the structural capacity of in-service asphalt pavements (30, 31). As expressed in Equation 1, the SNR is the ratio of the effective structural number (SN_{eff}) and the required structural number (SN_{req}) (17, 32). The SN_{eff} indicates the structural number of existing asphalt pavements, and the SN_{req} is the minimum structural number to ensure a desirable structural performance over the design period. Theoretically, the SN_{eff} should be greater than the SN_{req} to achieve adequate structural performance, and the minimum SNR requirement is one.

$$SNR = \frac{SN_{eff}}{SN_{req}} \quad (1)$$

The American Association of State Highway and Transportation Officials (AASHTO) 1993 pavement design guide dictates the methods to determine the SN_{eff} and SN_{req} using the FWD deflection data. The SN_{req} can be determined by solving Equation 2, and input parameters are a subgrade resilient modulus (M_R), equivalent single axle load (ESAL), reduction in serviceability (ΔPSI), standard deviation (S_0), and standard normal deviate (Z_R). In this study, the FWD deflection measured at 1,524 mm (60 in.) away from the loading center was used to calculate the M_R . It should be noted that upper layers (i.e., asphalt base layer) may affect deflections measured from nearer sensors (D48 or D36) because strong structures of full-depth asphalt pavements result in a wider stress zone. Thus, the D60 was selected to accurately estimate the M_R of full-depth asphalt pavements. The same ESAL was assumed for each road classification, based on the ESAL category dictated in the INDOT specification. The State Road used one million ESALs, while US-Highway and Interstate Highway used four million and 10 million ESALs, respectively. In addition, 1.701 of ΔPSI and 0.35 of S_0 , which are recommended in the INDOT specification, were used. The Z_R was determined based on the reliability levels following the AASHTO 1993 design guide: -1.037 for an 85% reliability level, -1.282 for a 90% reliability level, and -1.645 for a 95% reliability level. It should be noted that the same reliability levels used for the reliability analysis were applied to the SN_{req} calculation (i.e., State Road: 85%, US-Highway: 90%, and Interstate Highway: 95%).

$$\begin{aligned} \log ESAL &= Z_R \times S_0 + 9.36 \times \log(SN_{req} + 1) - 0.2 \\ &\quad + \frac{\log(\frac{\Delta PSI}{4.2-1.5})}{0.4 + \frac{1094}{(SN_{req} + 1)^{5.19}}} + 2.32 \times \log M_R - 8.07 \\ M_R &= \frac{0.24 \times P}{d_r \times r} \end{aligned} \quad (2)$$

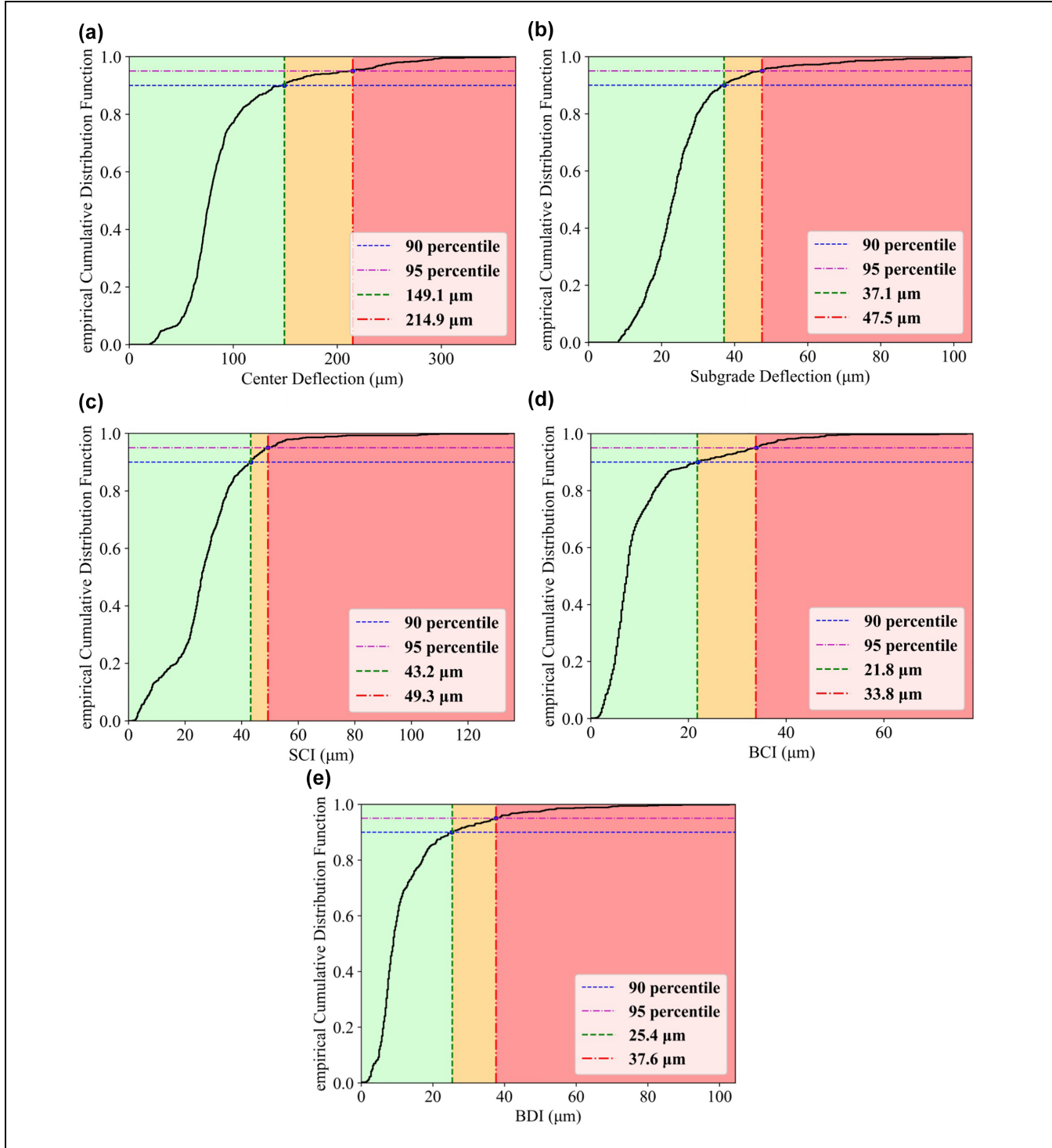


Figure 2. Empirical cumulative distribution function plot for falling weight deflectometer deflection parameters on Interstate full-depth asphalt pavement: (a) center deflection (D0), (b) subgrade deflection (D60), (c) surface curvature index (SCI), (d) base curvature index (BCI), and (e) base damage index (BDI).

where $ESAL$ is the equivalent single axle load, ΔPSI is a reduction in serviceability, S_0 is a standard deviation, Z_R is a standard normal deviate, M_R is a subgrade resilient

modulus (ksi), P is the FWD load (lbs.), r is a distance from the center of load (in.), and d_r is a deflection at a distance r from the center of the load (in.).

Table 1. Reliability Results of Falling Weight Deflectometer Deflection Parameters

Road type	Percentage (%)	D0 (microns)	D60 (microns)	SCI (microns)	BCI (microns)	BDI (microns)
State Road	80	359.9	59.4	111.0	57.2	81.5
	85	388.6	62.2	123.2	62.2	89.2
	90	423.7	67.3	138.7	68.1	102.9
	95	494.3	77.5	171.2	82.6	125.0
US-Highway	80	212.9	50.5	58.9	30.5	45.5
	85	227.6	53.1	66.0	34.3	50.0
	90	259.8	56.6	76.7	39.1	55.9
	95	295.4	63.0	94.0	46.2	68.6
Interstate Highway	80	106.4	30.2	35.6	13.2	17.3
	85	121.4	33.0	38.1	15.5	19.6
	90	149.1	37.1	43.2	21.8	25.4
	95	214.9	47.5	49.3	33.8	37.6

Note: BCI = base curvature index; BDI = base damage index; SCI = surface curvature index; Shaded cells = preliminary threshold values.

According to the AASHTO 1993 design guide, the SN_{eff} can be determined using the total pavement thickness and the effective modulus of existing pavements obtained from the FWD data. However, the AASHTO 1993 method requires a trial-and-error procedure to obtain the pavement effective modulus, which is a key parameter for SN_{eff} calculation and is impractical to be incorporated into the network-level PMS. Furthermore, the AASHTO 1993 method is significantly dependent on the pavement thickness, resulting in overestimated SN_{eff} . Thus, previous researchers have developed alternative models to estimate the SN_{eff} using the FWD deflection data, without a trial-and-error procedure (9, 17, 33). Recently, a new SN_{eff} prediction model was developed and verified with field data in a concurrent study conducted by INDOT. As expressed in Equation 3, the new model only requires a total pavement thickness and the FWD deflection basin parameter, the area under pavement profile (*AUPP*), to make accurate predictions of SN_{eff} . Therefore, this study adopts this new model to calculate the SN_{eff} .

$$SN_{eff} = 2.272 \times H_p^{0.4217} \times AUPP^{-0.4678} \quad (3)$$

where H_p is the pavement thickness above subgrade (in.), and *AUPP* is the area under pavement profile (mils).

The maximum FWD deflection D0 was selected as a representative FWD parameter to compare with the preliminary threshold values calculated using reliability analysis as both D0 and SNR represent the overall structural conditions of existing pavements. Other FWD parameters are typically used to estimate the structural conditions of specific layers (i.e., surface layer, base layer, and subgrade layer), indicating that a different

more specific structural index may be needed to compare with the other FWD parameters. However, there are currently no available structural indices for individual layers. Therefore, the reliability-based approach was extended to the other FWD parameters to determine the final threshold values if the D0 thresholds match with thresholds calculated from SNR.

Figure 3 shows that the SNR decreased as D0 increased with an exponential relationship, for all road classifications, including State Roads, US-Highways, and Interstate Highways. Based on the relationship, the D0 values, corresponding to the SNR limit were identified to establish the D0 threshold range for each road classification. As shown in Figure 3, the D0 threshold of State Roads ranged from 125 to 400 microns, and the D0 threshold range was 120 to 254 microns for US-Highways and 100 to 203 microns for Interstate Highways, respectively. Overall, the threshold of State Roads was greater than the threshold of Interstate Highways. This trend is consistent with the standard pattern and was also observed in reliability-based threshold values. Interestingly, for all road classifications, the upper limit of the threshold range was almost identical to highlighted D0 threshold value from the reliability analysis in Table 1. For example, the upper limit of the reliability-based threshold of D0 for State Road (388.6 microns) was slightly smaller than the upper limit of the D0 threshold identified based on the SNR analysis (400 microns). Therefore, the threshold calculated from the reliability analysis of current road conditions was verified with a similar threshold range obtained from SNR calculation. Therefore, it was used to distinguish good, fair, and poor structural conditions of full-depth asphalt pavements, and the final threshold values of FWD deflection parameters are presented in Table 2.

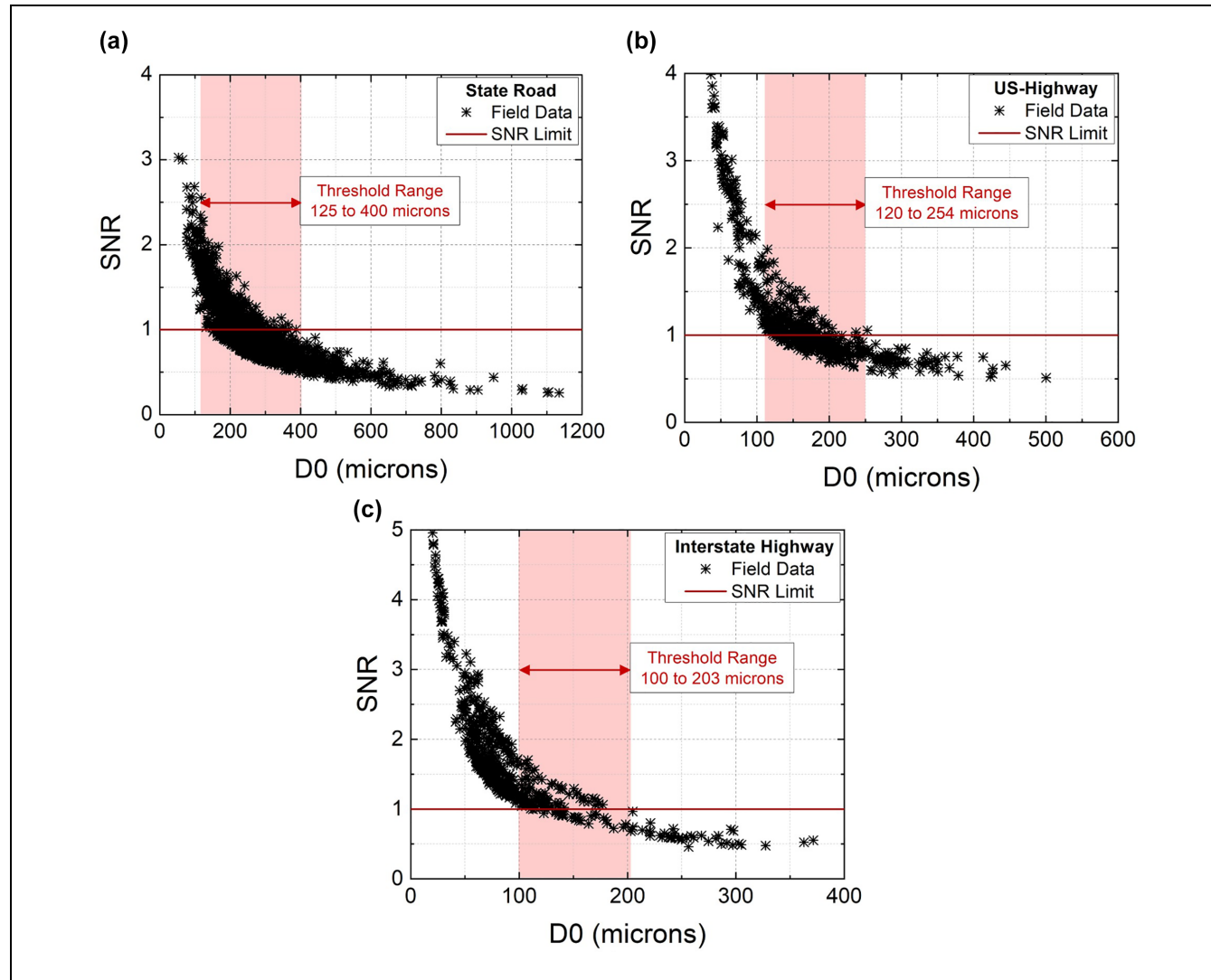


Figure 3. Comparison between structural number ratio (SNR) and D0: (a) State Road, (b) US-Highway, and (c) Interstate Highway.

Table 2. Final Threshold Values of FWD Deflection Parameters

Road type	FWD parameter	Good	Fair	Poor
State Road	D0 (microns)	$D0 < 359.9$	$359.9 < D0 < 388.6$	$388.6 < D0$
	D60 (microns)	$D60 < 59.4$	$59.4 < D60 < 62.2$	$62.2 < D60$
	SCI (microns)	$SCI < 111.0$	$111.0 < SCI < 123.2$	$123.2 < SCI$
	BCI (microns)	$BCI < 57.2$	$57.2 < BCI < 62.2$	$62.2 < BCI$
	BDI (microns)	$BDI < 81.5$	$81.5 < BDI < 89.2$	$89.2 < BDI$
US-Highway	D0 (microns)	$D0 < 227.6$	$227.6 < D0 < 259.8$	$259.8 < D0$
	D60 (microns)	$D60 < 53.1$	$53.1 < D60 < 56.6$	$56.6 < D60$
	SCI (microns)	$SCI < 66.0$	$66.0 < SCI < 76.7$	$76.7 < SCI$
	BCI (microns)	$BCI < 34.3$	$34.3 < BCI < 39.1$	$39.1 < BCI$
	BDI (microns)	$BDI < 50.0$	$50.0 < BDI < 55.9$	$55.9 < BDI$
Interstate Highway	D0 (microns)	$D0 < 149.1$	$149.1 < D0 < 214.9$	$214.9 < D0$
	D60 (microns)	$D60 < 37.1$	$37.1 < D60 < 47.5$	$47.5 < D60$
	SCI (microns)	$SCI < 43.2$	$43.2 < SCI < 49.3$	$49.3 < SCI$
	BCI (microns)	$BCI < 21.8$	$21.8 < BCI < 33.8$	$33.8 < BCI$
	BDI (microns)	$BDI < 25.4$	$25.4 < BDI < 37.6$	$37.6 < BDI$

Note: BCI = base curvature index; BDI = base damage index; FWD = falling weight deflectometer; SCI = surface curvature index.

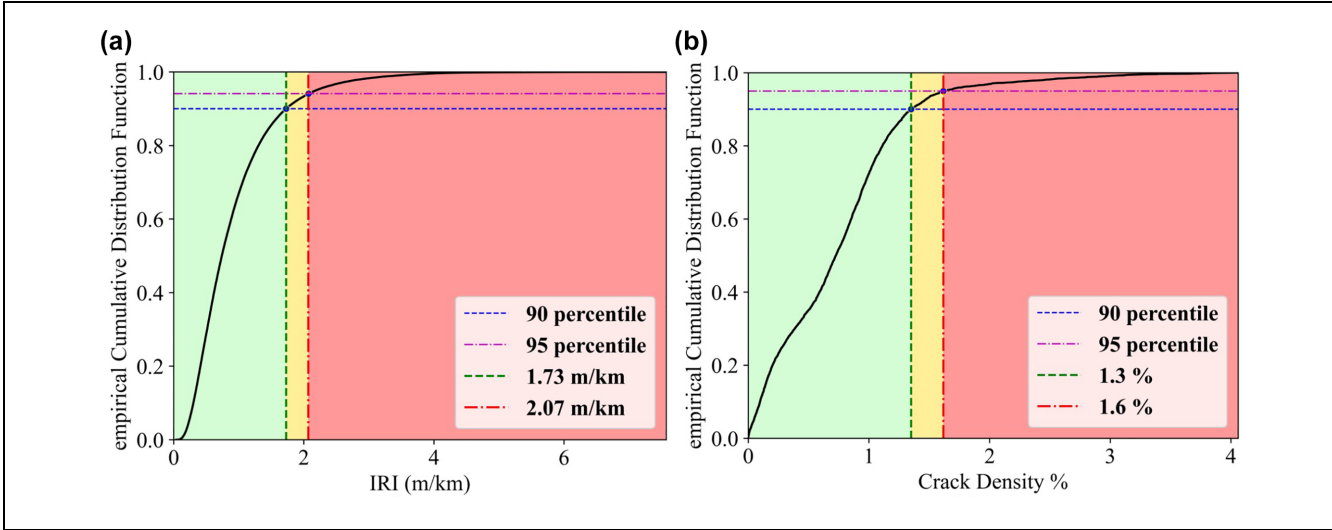


Figure 4. Empirical cumulative distribution function plot for functional parameters of Interstate Highway: (a) international roughness index (IRI) and (b) crack density (CD).

Determination of Functional Parameters Thresholds

Thresholds of IRI and CD were determined using the reliability percentile values verified by the threshold comparison results of FWD deflection parameters. Figure 4 shows ECDF plots of IRI and CD for Interstate Highway. The 95% and 90% reliability levels were used for rating the pavements into good, fair, and poor conditions. Accordingly, the higher IRI threshold value was 2.07 m/km, and the lower IRI threshold value was 1.73 m/km. Similarly, the higher threshold of CD was 1.3%, whereas the lower threshold value for CD was 1.6%. It is important to note that thresholds of IRI and CD were determined only for full-depth asphalt pavement and Interstate Highways, as IRI and CD data collection is ongoing for State Roads and US-Highways. Thus, in this study, Interstate Highway was used to verify the concept and algorithm for patching suggestions.

Evaluation of Pavement Condition Rating Parameters

Comparison of Overall Road Conditions

Interstate Highway I-70 was used as a representative full-depth asphalt pavement to determine the utility of PCR parameters in assessing overall road conditions. The overall conditions of the driving lane (DL) and passing lane (PL) for both eastbound (EB) and westbound (WB) roads were analyzed using central tendency plots shown in Figure 5, by comparing their mean and median values. Here, the red dots are points in the high severity range which represent road locations in poor condition, the yellow dots are in the medium severity range, that is, locations with fair road conditions, and the green dots

are in the low severity range, that is, locations with good road conditions. Thus, the red and yellow point markers represent the PCR parameter measurements at locations which were selected as candidates for maintenance by the patching suggestion algorithm. The black quadrilaterals and black horizontal lines are the mean and median of the PCR parameters on the plotted road sections. Overall, this plot shows that both right-wheel IRI and left-wheel IRI values of the driving lane are greater than those in the passing lane for both EB and WB, illustrated by their comparatively higher mean and median values. Usually, a driving lane has more wear than a passing lane, because of the higher traffic volume on the driving lane. This indicates that the functional parameters can correctly compare the overall functional condition of lanes using the central tendency parameters and detect road locations which require attention.

As shown in Figure 6, *a* and *b*, a similar trend was observed from D0 and D60 on the same road section on I-70. Both the D0 and D60 values of the driving lane were greater than the passing lane based on the central tendency parameters. As expected, the driving lane results exhibited higher variations in both D0 and D60 compared with passing lane results, represented by higher mean and median values and significantly high deflection measurements. Higher traffic density on driving lanes exacerbates the pavement stress, causing greater deflection values and increased variation in the distribution of D0 and D60. In addition to the overall road/lane comparison, the box plot in Figure 6c draws the comparison of FWD deflection parameters across the road classifications. Here, the bottom edge of the rectangle denotes the first quantile (25%) mark, and the upper edge of the rectangle denotes the third quantile (75%)

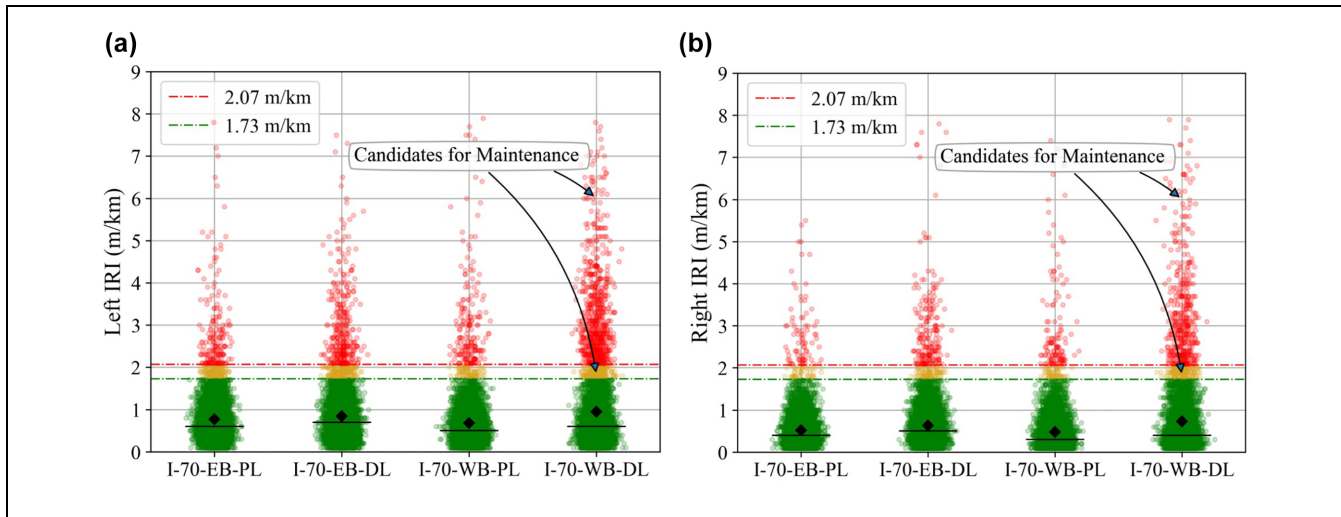


Figure 5. Comparison of international roughness index (IRI) on I-70: (a) left IRI and (b) right IRI.

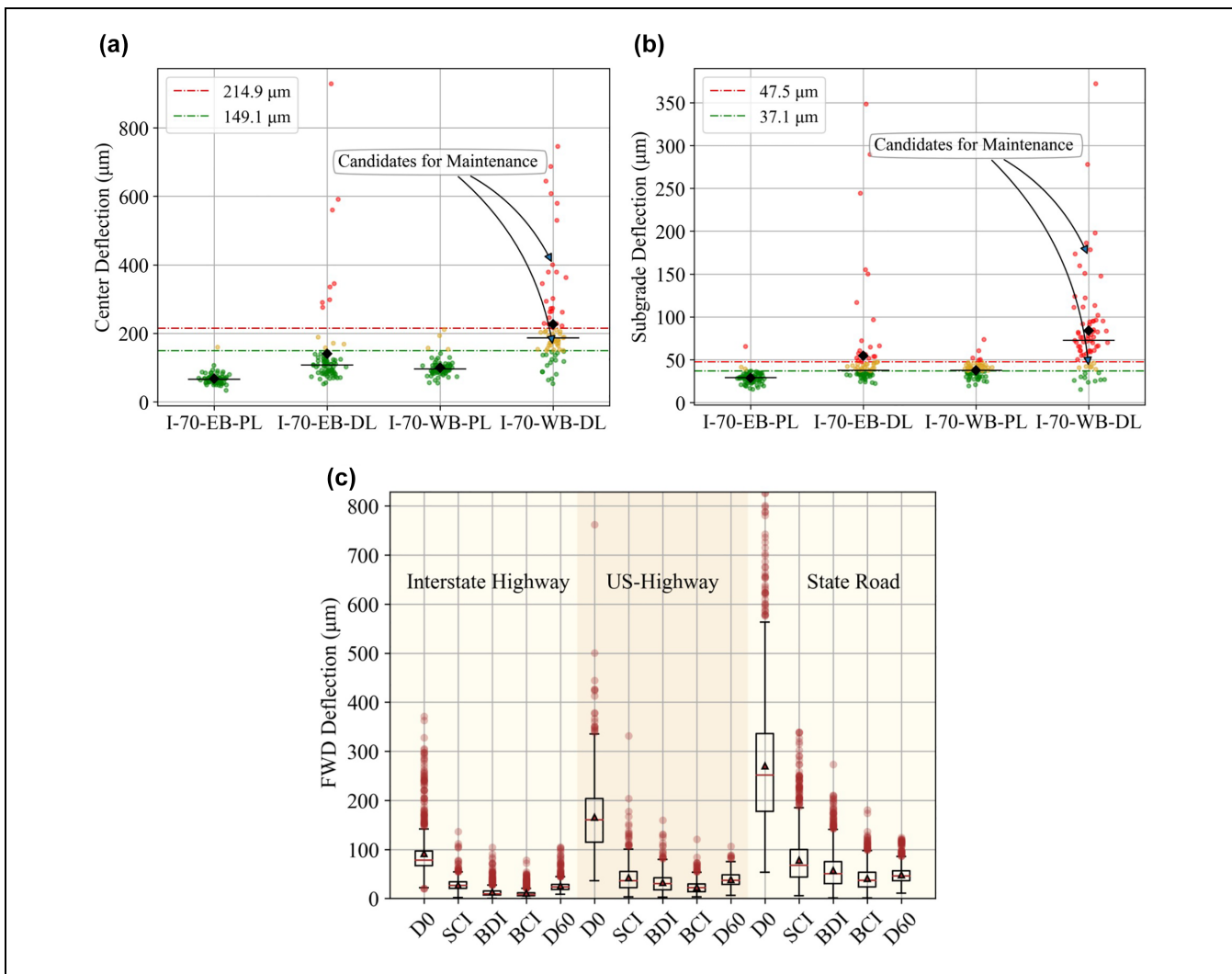


Figure 6. Comparison of falling weight deflectometer (FWD) parameters: (a) center deflection D0 of I-70, (b) subgrade deflection D60 of I-70, and (c) all FWD deflection parameters from all road classifications. Here the Y-axis ranges of (a) and (b) are different to conserve the necessary information in both figures.

mark in the PCR parameter measurements. The mean of these data is represented by the black triangle and the median by the brown horizontal line. The length of the black vertical lines denotes the range of the data, and the minimum and maximum values are shown at the edges of these lines. The brown point markers represent the possible outliers in the dataset. As Interstate Highway is typically designed with stronger pavement structures to support a heavier traffic volume, overall FWD deflection parameters are lower than on US-Highways and State Roads. This means that the FWD deflection parameters can be used as structural indicators to represent overall road conditions.

Identifying Localized Distresses Using PCR Parameters

Identifying localized distresses is the major expectation from the PCR parameters in providing accurate geolocation of road sections with maintenance requirements. Spatially integrated IRI and FWD deflection parameters were compared with the CD, road surface, and ROW images to determine whether these parameters can successfully capture the localized distresses of in-service full-depth asphalt pavements. A stem plot comparison of the three PCIs at each DMI number for the same section of I-70 as in the previous section is shown in Figure 7. The highest value of L-IRI, 8.1 m/km was observed at the left wheel path DMI 2922, on I-70-WB-PL as shown in the plot in Figure 7a. This value is also greater than the interstate IRI threshold value.

The road surface and ROW images of the same DMI number 2922 captured from the WayLink software show localized patching for pothole on the left edge of the road, marked with a red arrow in Figure 7b. Similarly, left and right IRI values, R-IRI 7.7 m/km and L-IRI 5.4 m/km, were greater than the IRI threshold value at DMI 330. The high L-IRI value is shown in the stem plot in Figure 7c. A strip patching was captured at DMI number 330 on the same section of I-70 as shown in Figure 7d. As shown in Figure 7, e and f, the authors were also able to locate DMI with a high center deflection on the I-70 westbound road. A center deflection value of 280 microns was captured at this DMI 47230, which is higher than the calculated threshold value, and cracks are easily visible on the road surface and ROW images in the WayLink software. The authors have extensively checked the ability of the 1.8 m-resolution data to detect localized distresses by selecting assessment index values exceeding their upper threshold values from scatter plots and comparing them with their corresponding ROW image and road surface image. These findings confirm that the selected PCR parameters accurately detected localized distresses and other features on roads such as crack sealing, small patching, uphill, downhill,

turns, railroad crossings, and so forth, from road condition parameter data alone.

Development of PMT

Patching Suggestion Algorithm

Pavement surface patching and full-depth patching were used as the patching depth suggestions in the surface condition evaluation. Surface patching and full-depth patching are defined according to the AASHTO pavement maintenance protocol. Patching required and patching warning was similarly used as patching priority suggestion. Patching required has higher priority in maintenance than patching warning. Figure 8 illustrates the classification of the state of the three pavement layers into five conditions for patching. The underlying rectangular shapes represent the surface, base/intermediate and sub-base/subgrade layers of a full-depth asphalt pavement. The red, orange, and green colored layers represent the current state of the layers. Green represents the good state of layers, that is, values lower than the lower thresholds of PCRs, orange represents the fair state, and red represents the poor state of pavement layers, that is, PCR values greater than the upper thresholds calculated earlier.

Condition 1 shows the poor condition of the sub-base/subgrade layer with a combination of the poor state of the intermediate/base layer. Pavement in this state requires a full-depth patch regardless of the condition of the surface layer. Similarly, when the intermediate/base layer is in a poor state and the sub-base/subgrade layer is in a fair state, *Condition 2* would be applicable and a warning for full-depth patching would be suggested by the algorithm. Furthermore, the patching suggestion requirement and warning for surface patching are based on two combinations of pavement layer states as shown in *Conditions 3* and *4*. *Condition 3* requires surface layer patching determined by the poor condition of the surface layer with fair state of the base/intermediate layer and good condition of the sub-base/subgrade layer. *Condition 4* indicates warning surface layer patching determined by the fair state of the surface layer and good conditions of base/intermediate and sub-base/subgrade layers. Lastly, *Condition 5* indicates good road conditions where no further action is needed. This conditional patching suggestion algorithm is reinforced by adding pavement type/road classification threshold values. The threshold-based patching suggestion for Interstate Highway full-depth asphalt pavement is aggregated in Table 3.

Web-Based Application: PMT

A web-based application can be hosted on an internet browser and thus is easily available to view with

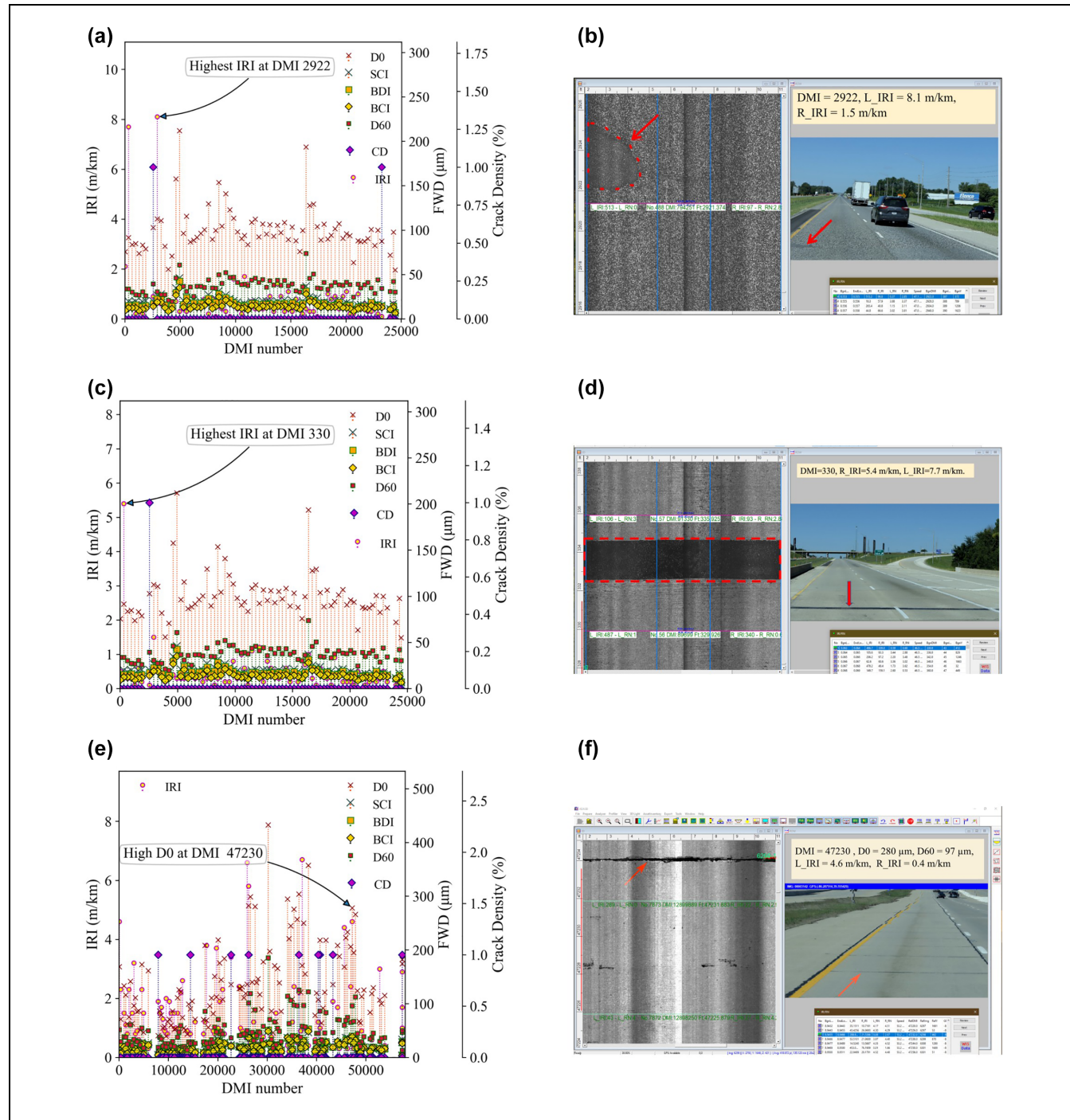


Figure 7. Comparison of IRI, FWD deflections and CD using stem plots and scoping for faults using ROW image and road surface image at selected DMI on different sections of I-70: (a) stem plot at DMI 2922, (b) ROW and road surface image at DMI 2922, (c) stem plot at DMI 330, (d) ROW and road surface image at DMI 330, (e) stem plot at DMI 47230, and (f) ROW and road surface image at DMI 47230. Note: CD = crack density; FWD = falling weight deflectometer; IRI = international roughness index; ROW = right-of-way.

credentials. The open-source structure of the application also makes it free to use for individual analysts/engineers. In the PMT application, the threshold-based patching algorithm is currently implemented using the spatially indexed and integrated PCR parameters to

create patching suggestions for roads of interest. Using the application, patching suggestions can be downloaded which include location coordinates, PCR parameter measurement values, suggested parameter severity ratings, patching information (i.e., area, depth, quantity,

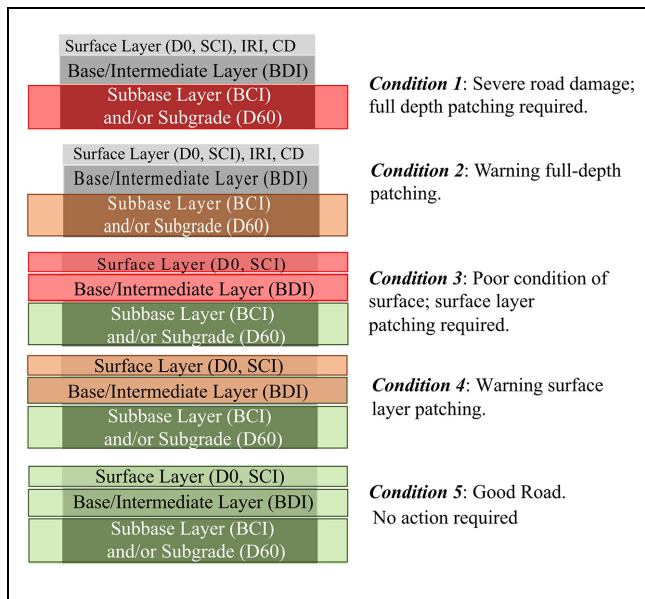


Figure 8. Patching conditions labeled according to the measurement range of falling weight deflectometer deflections.
 Note: BCI = base curvature index; BDI = base damage index; CD = crack density; IRI = international roughness index; SCI = surface curvature index.

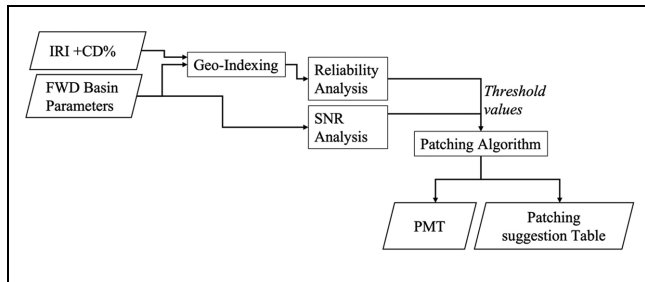


Figure 9. The flow diagram of processing the raw data for Patching Management Tool.
 Note: CD = crack density; FWD = falling weight deflectometer; IRI = international roughness index; PMT = Patching Management Tool; SNR = structural number ratio.

and priority suggestion), and pavement information (i.e., road name, pavement type, reference point, and lane). Figure 9 illustrates a block diagram which shows the flow diagram of processing the raw data till publishing it on PMT.

The developed web application has three major functionalities. Once a road of interest is selected, it creates a table with patching location and quantity suggestions, which is presented as color-coded visualization on the geographical map of Indiana. Colored markers are used to represent pavement sections of 1.8 m in length and 3.6 m in width, as shown in Figure 10. These markers are identified by unique DMI numbers and geographical coordinates. The marker color represents patching depth

Table 3. Threshold-Based Patching Suggestion Algorithm for Interstate Full-Depth Asphalt Pavement

IRI (m/km)	CD (%)	D0 (μm)	SCI (μm)	BDI (μm)	D60 (μm)	BCI (μm)	Patching suggestions
NA	NA	NA	NA	NA	> 47.5	> 33.8	Severe road damage; full-depth patching requirement
NA	NA	NA	NA	> 37.1 & ≤ 47.5	> 21.8 & ≤ 33.8	Full-depth patching warning	Poor condition of surface layer; surface patching required
> 2.07	> 13.2	> 49.3	> 37.6	≤ 37.1	≤ 21.8	Surface patching warning	No action required
> 1.73 & ≤ 2.07	> 12.5 & ≤ 13.2	> 149.1 & ≤ 214.9	> 43.2 & ≤ 49.3	> 25.4 & ≤ 37.6	≤ 37.1	≤ 21.8	
≤ 1.73	≤ 12.5	≤ 149.1	≤ 43.2	≤ 25.4	≤ 37.1	≤ 21.8	

Note: BCI = base curvature index; BDI = base damage index; CD = crack density; IRI = international roughness index; SCI = surface curvature index; NA = not applicable; Red cells = poor state; Orange cells = fair state; Green cells = good state.



Figure 10. Web-based Patching Management Tool: (a) patching suggestion for the example road I-69 using color-coded markers and graphs for analysis of parameters, and (b) user input threshold selector for patching suggestion calculation with an example patching table.

and priority. For example, the red markers represent high-priority full-depth patching requirements, the orange markers mean a warning for a full-depth patch, the yellow markers warn that a surface patch may be needed, and the green marker represents good road locations.

The PMT also supports distress data analysis features, which include histogram analysis and scatter plot analysis of pavement rating parameters. These analysis tools

are necessary to analyze the values at the location nearest to distress to understand its probable causes. The causes of distress are crucial factors in determining the maintenance suggestions. The potential of the web application is placed in its data-driven ability to allow users to compare road conditions at distressed locations which may be miles apart.

To verify the developed web-based PMT application, the patching suggestions provided by PMT were

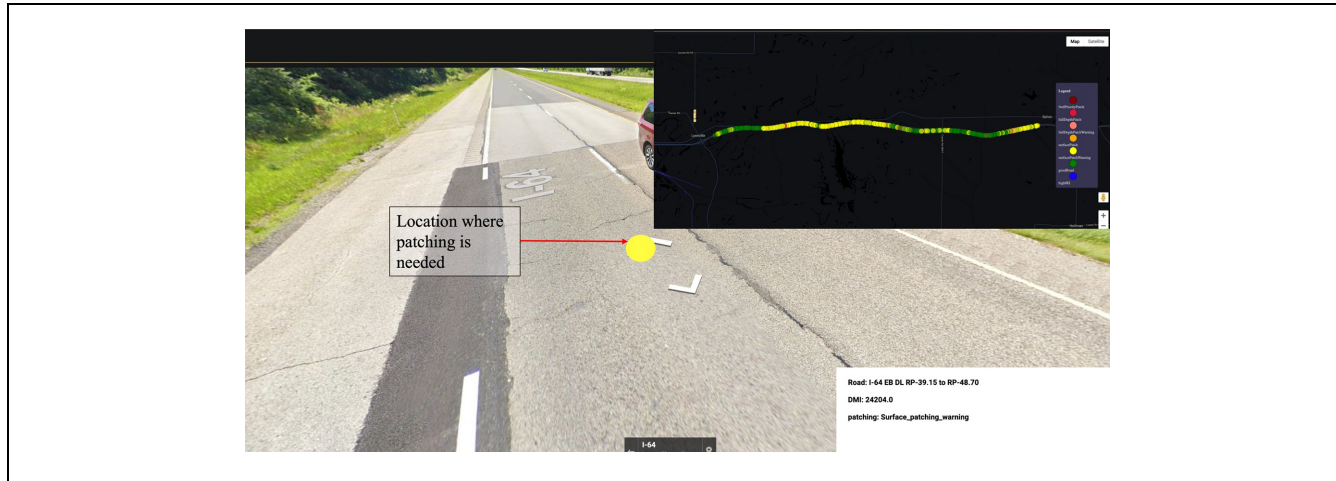


Figure 11. Example of the final output of patching suggestion in Patching Management Tool.

compared with the Google Street View feature in PMT. An example of a road, I-64 was used for this verification. A particular DMI 24204 on I-64 EB DL is shown in Figure 11, which was selected from the patching suggestion visualization, and the street view at this DMI was explored. PMT suggests a warning for surface patching at DMI 24204 shown with a yellow marker because the IRI at this location was greater than its lower threshold value. Therefore, it was confirmed that PMT accurately suggests patching suggestions at genuinely distressed locations, also captured in the Google Street View map.

Conclusion

This study proposes a reliability-SNR-based threshold calculation method for integrated PCR parameters. The data fusion approach integrating structural and functional assessment parameters with the matched geographical location describes the overall pavement assessment with better accuracy. It considers roughness, cracking, and FWD deflections at the same location, allowing the automation of improved patching suggestions. The patching suggestion algorithm incorporates the overall pavement condition information and can create five pavement condition ratings based on the distress level in three major layers of the pavement structure. The algorithm was tested using calculated PCR parameter threshold values for Interstate full-depth asphalt pavement segments. Comparative analysis of PCR parameters was able to detect localized distresses. This could reduce the bulk human resource and time required in a manual routine survey. The developed threshold-based patching suggestion algorithm was reinforced with a web-based application, PMT, to assist in the current practices of

PMS. The key features of the web-based PMT application are summarized below:

- The web application plots comprehensive patching suggestions with color-coded markers for a selected road segment on a map.
- PMT integrates two-dimensional road surface and ROW images to aid visual field assessments.
- PMT allows users to take advantage of Google Street View at the patching locations for 3D virtual spatial analysis.
- Histogram and scatter plots are included to analyze the distribution or pattern in PCR parameters along/among the selected roads.
- PMT supports the manual adjustment of threshold values for each PCR parameter in the patching suggestion algorithm. This feature creates flexibility for users to customize the patching tables, which are essential for analyzing and updating maintenance standards.

The PMT web-based application can provide a high-resolution comprehensive patching suggestion with key features summarized above, and was successfully verified with ROW images and Google Street View map. Furthermore, this study introduced the approach to determine appropriate threshold values based on local road conditions, and this approach can be used for roads in other states or countries. Consequently, the PMT web-based application, along with the proposed approach for threshold determination, can be applied to any region with different road conditions.

As a next step, ground-penetrating radar and traffic speed deflectometer will be included as additional PCR parameters to improve the accuracy and increase the resolution of patching depth suggestions. In addition, the

database structure in PMT web-based application will be scaled up to display and analyze larger datasets such as statewide road network on a map simultaneously. Moreover, additional field performance data will be collected to further validate the determined threshold values.

Acknowledgment

We would like to thank Dr. Kelvin Wang and Dr. Guangwei Yang at Oklahoma State University for assisting with WayLink systems corporation 3D imaging software.

Author Contributions

The authors confirm their contribution to the paper as follows: study conception and design: Seonghwan Cho, James V. Krogmeier, and John E. Haddock; data collection: Bongsuk Park; analysis and interpretation of results: Seonghwan Cho, James V. Krogmeier, John E. Haddock, Sneha Jha, Yaguang Zhang, and Bongsuk Park; draft manuscript preparation: Seonghwan Cho, James V. Krogmeier, John E. Haddock, Sneha Jha, Yaguang Zhang, and Bongsuk Park. All authors reviewed the results and approved the final version of the manuscript.

Declaration of Conflicting Interests

The author(s) declared no potential conflicts of interest with respect to the research, authorship, and/or publication of this article.

Funding

The author(s) disclosed receipt of the following financial support for the research, authorship, and/or publication of this article: This work was supported in part by the Joint Transportation Research Program administered by the Indiana Department of Transportation and Purdue University [SPR-4521].

ORCID iDs

Yaguang Zhang  <https://orcid.org/0000-0002-5445-0555>
 Bongsuk Park  <https://orcid.org/0000-0003-4606-4408>
 James V. Krogmeier  <https://orcid.org/0000-0001-7041-2113>
 John E. Haddock  <https://orcid.org/0000-0002-8030-317X>

References

- Kulkarni, R. B., and R. W. Miller. Pavement Management Systems: Past, Present, and Future. *Transportation Research Record*, 2003. 1853(1): 65–71.
- Wolters, A. S., and K. A. Zimmerman. *Current Practices in Pavement Performance Modeling*. Applied Pavement Technology, Urbana, IL, 2010. FHWA-PA-2010-007-080307.
- Baladi, G. Y., M. Prohaska, K. Thomas, T. Dawson, and G. Musunuru. *Pavement Performance Measures and Forecasting and the Effects of Maintenance and Rehabilitation Strategy on Treatment Effectiveness (Revised)*. Federal Highway Administration, McLean, VA, 2017. FHWA-HRT-17-095.
- Haider, S. W., K. Chatti, G. Y. Baladi, and N. Sivaneswaran. Impact of Pavement Monitoring Frequency on Pavement Management System Decisions. *Transportation Research Record*, 2011. 2225(1): 43–55.
- Lamptey, G., M. Z. Ahmad, S. Labi, and K. C. Sinha. *Life Cycle Cost Analysis for INDOT Pavement Design Procedures*. Purdue University Press, West Lafayette, Indiana, 2005.
- Pedigo, R. D., F. L. Roberts, W. R. Husdon, and R. C. Haas. Pavement Management: The Network-Level Decision Process. Application of Pavement Design. In *59th Annual Meeting of the Transportation Research Board*, Washington, D. C., 1979.
- Chikezie, C. U., A. T. Olowosulu, and O. S. Abejide. Multiobjective Optimization for Pavement Maintenance and Rehabilitation Programming using Genetic Algorithms. *Archives of Applied Science Research*, Vol. 5, No. 4, 2013, pp. 76–83.
- Ismail, N., A. Ismail, and R. Atiq. An Overview of Expert Systems in Pavement Management. *European Journal of Scientific Research*, Vol. 30, No. 1, 2009, pp. 99–1119.
- Kavussi, A., M. Abbasghorbani, F. Moghadas Nejad, and Z. A. Bamdad. A New Method to Determine Maintenance and Repair Activities at Network-Level Pavement Management Using Falling Weight Deflectometer. *Journal of Civil Engineering and Management*, Vol. 23, No. 3, 2017, pp. 338–346.
- McDaniel, R., J. Olek, A. Behnood, B. Magee, and R. Pollock. *Pavement Patching Practices*. Transportation Research Board, Washington, D. C., 2014.
- Setiaputri, H. A., M. Isradi, A. I. Rifai, A. Mufhidin, and J. Prasetijo. Analysis Of Urban Road Damage With Pavement Condition Index (PCI) And Surface Distress Index (SDI) Methods. *ADRI International Journal of Sciences, Engineering and Technology*, Vol. 6, No. 1, 2021, pp. 10–19.
- Bryce, J., R. Boadi, and J. Groeger. Relating Pavement Condition Index and Present Serviceability Rating for Asphalt-Surfaced Pavements. *Transportation Research Record*, 2019. 2673(3): 308–312.
- Sidess, A., A. Ravina, and E. Oged. A Model for Predicting the Deterioration of the Pavement Condition Index. *International Journal of Pavement Engineering*, 2021. 22(13): 1625–1636.
- Gkyrtis, K., A. Loizos, and C. Plati. Integrating Pavement Sensing Data for Pavement Condition Evaluation. *Sensors (Basel)*. Vol. 21, No. 9, 2021, p. 3104.
- Rada, G. R., R. W. Perera, V. C. Prabhakar, and L. J. Wiser. Relating Ride Quality and Structural Adequacy for Pavement Rehabilitation and Management Decisions. *Transportation Research Record*, Vol. 2304, No. 1, 2012, pp. 28–36.
- Lytton, R. L. *Backcalculation of Pavement Layer Properties*. ASTM International, West Conshohocken, Pennsylvania, 1989.
- Rohde, G. T. Determining Pavement Structural Number from FWD Testing. *Transportation Research Record*, 1994. 1448: 61–68.

18. Sollazzo, G., T. Fwa, and G. Bosurgi. An ANN Model to Correlate Roughness and Structural Performance in Asphalt Pavements. *Construction and Building Materials*, Vol. 134, 2017, pp. 684–693.
19. Xiao, M., R. Luo, and X. Yu. Assessment of Asphalt Pavement Overall Performance Condition Using Functional Indexes and FWD Deflection Basin Parameters. *Construction and Building Materials*, Vol. 341, 2022, p. 127872.
20. Horak, E., A. Hefer, S. Emery, and J. Maina. Flexible Road Pavement Structural Condition Benchmark Methodology Incorporating Structural Condition Indices Derived from Falling Weight Deflectometer Deflection Bowls. *Journal of Civil engineering and Construction*, Vol. 4, No. 1, 2015, pp. 1–14.
21. Wang, K. C. P., Z. Hou, and S. Williams. Precision Test of Cracking Surveys with the Automated Distress Analyzer. *Journal of Transportation Engineering*, Vol. 137, No. 8, 2011, pp. 571–579.
22. Wang, K. C., J. Q. Li., and G. Yang. *Waylink ADA3 Software*. 3rd ed. Oklahoma State University, Stillwater, 2021.
23. Zhang, A., K. C. P. Wang, B. Li, E. Yang, X. Dai, and Y. Peng. Automated Pixel-Level Pavement Crack Detection on 3D Asphalt Surfaces Using a Deep-Learning Network. *Computer-Aided Civil and Infrastructure Engineering*, Vol. 32, No. 10, 2017, pp. 805–819.
24. Park, B., S. Cho, R. Rahbar-Rastegar, T. E. Nantung, and J. E. Haddock. Prediction of Critical Responses in Full-Depth Asphalt Pavements using the falling Weight Deflectometer Deflection Basin Parameters. *Construction and Building Materials*, Vol. 318, 2022, p. 126019.
25. AASHTO. *Mechanistic-Empirical Pavement Design Guide: A Manual of Practice*. AASHTO, Washington, D. C., 2020.
26. AASHTO. *AASHTO Guide for Design of Pavement Structures*. AASHTO, Washington, D. C., 1993.
27. Bryce, J., G. W. Flintsch, S. W. Katicha, and B. K. Diefenderfer. *Developing a Network-Level Structural Capacity Index for Structural Evaluation of Pavements*. Virginia Center for Transportation Innovation and Research, Washington, D. C., 2013.
28. Flora, W. F., G. P. R. Ong, and K. C. Sinha. *Development of a Structural Index as an Integral Part of the Overall Pavement Quality in the INDOT PMS*. Purdue University Press, West Lafayette, Indiana, 2010.
29. U.S. Department of Transportation/Federal Highway Administration. *Transportation Performance Management [Internet]*. <https://www.fhwa.dot.gov/tpm/reporting/state/reliability.cfm?state=Indiana>. Accessed November 20, 2022.
30. Zhang, Z., G. Claros, L. Manuel, and I. Damnjanovic. Development of Structural Condition Index to Support Pavement Maintenance and Rehabilitation Decisions at Network Level. *Transportation Research Record*, 2003. 1827(1): 10–17.
31. Kim, M. Y., D. Y. Kim, and M. R. Murphy. Improved Method for Evaluating the Pavement Structural Number with Falling Weight Deflectometer Deflections. *Transportation Research Record*, 2013. 2366(1): 120–126.
32. Abd El-Raof, H. S., R. T. Abd El-Hakim., S. M. El-Badawy, and H. A. Afify. Structural Number Prediction for Flexible Pavements Using the Long Term Pavement Performance Data. *International Journal of Pavement Engineering*, 2020. 21(7): 841–855.
33. Crook, A. L., S. R. Montgomery, and W. S. Guthrie. Use of Falling Weight Deflectometer Data for Network-Level Flexible Pavement Management. *Transportation Research Record*, 2012. 2304(1): 75–85.

This paper's contents reflect the views of the authors, who are responsible for the facts and accuracy of the data presented and do not necessarily reflect the official views or policies of the sponsoring organizations. These contents do not constitute a standard, specification, or regulation.